DESIGN AND MODELLING OF MINIATURIZED INVERTED E-SHAPED TEXTILE ANTENNA FOR ISM APPLICATIONS

Dr.K.Prasad [1], S.Imran Basha [2], Y.KEERTHI [3]

D.S.IFSHA TABASSUM [4].

1-Associate Professor, Dept of ECE, AITS, Rajampet, AP, India

2,3,4-Student, Dept of ECEE, AITS, Rajampet, AP, India

ABSTRACT

The issue of reducing the size of antennas is paramount for specific ISM applications. Wearable devices have become more significant over the past decade. There are many approaches already existed and used to decrease the size of a Patch antenna. It is optimized to operate at 2.4GHz using CST studio suite software. In order to improvise its operating performance, in this project the removal of proper rectangular slots and insertion of strip lines are the prime steps to decrease size of antenna. Almost the antenna size is 75% smaller than a conventional antenna. Each space and strip row is converted into their equivalent circuit and then merged to form the entire equivalent network of the antenna presented. Finally the expected qualitative analysis of the proposed inverted E-shaped textile antenna can achieve an improvement of size miniaturization of 30*20*0.7 mm^3 and demonstrates an impedance bandwidth of 15% and

efficiency of 79%, showing that it is a promising candidate for assimilation into wearable systems.

Keywords: miniaturized antenna, antenna slots, ISM band, microstrip and textile antenna.

1.INTRODUCTION

1.1ANTENNA MINIATURIZATION

Miniaturization of antennas has been the topic of various studies for nearly decades. Early studies showed a decrease in size of an antenna leading to a direct decrease in its bandwidth and performance. The size constraint translates into a lower limit on the achievable radiation quality factor and consequently on the overall impedance bandwidth attainable.

Recently, a variety of studies have been undertaken to minimize the form factor of various types of antennas while attempting to preserve appropriate matching properties and operational bandwidth. These miniaturization methods are usually related to modification of the electrical and physical properties of an atenna.

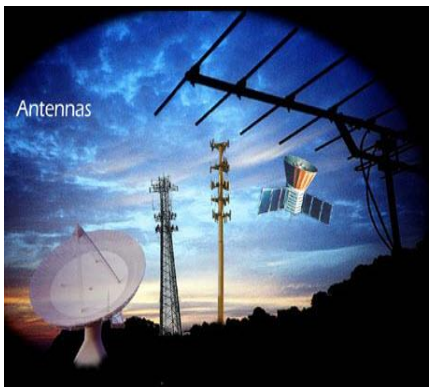

Fig 1. Various antennas used in different applications of communication systems

Wheeler suggested the ESA Electrically SmallAntenna, which is characterized as an antenn a with a maximum dimension of less than ג /2π , referred to as radian length.

Another widely used definition of an ESA is an antenna that satisfies the condition ka < 0.5, where k is the wave number 2π/ג, and ' a ' is the radius of the minimum size sphere that encloses the antenna as seen in Figure No.6, that sphere is referring to as "chu sphere".

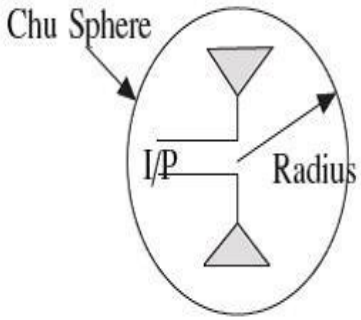

Figure No.2 : Biconical small antenna

1.1 DESIGN CRITERIA FOR MINIATURIZATION

As we learned, mobile terminals must be compact, small and energy-efficient. Nevertheless, the growth of the chip industry has enabled significant reductions in microelectronics and CPU computation over the last decade. On the other hand, miniaturization of the antenna has been a recent priority. The principle of miniaturization involves the the phase velocity of the signal, driven by the configuration of the antenna, to the specified resonance when the antenna is electrically low. To demonstrate how this can be done, we use the analog between the antenna and the transmission wire. Imagine a center fed infinite biconical antenna, a kind of spherically circular waveguide directing the spherical wave.

This is similar to the infinitely long, continuous transmission line that drives a plane wave. The phase velocity vp and the characteristic impedance Zo seen by the directed wave are given

$$v_p = \frac{1}{\sqrt{LC}} = \frac{1}{\sqrt{\mu\varepsilon}}, Z_0 = G\sqrt{\frac{L}{C}} = G\sqrt{\frac{\mu}{\varepsilon}}$$

While L is a series inductance per unit length, C is a shunt capacitance per unit length, and G is a geometric component. Phase velocity can therefore be adjusted using series inductance and shunt capacitance per unit length of the antenna. In the case of biconical antenna, sufficient electrical delay can be accomplished by controlling the self-inductance of the cone and the capacitance between the cone halves.

1.3 MINIATURIZATION OF PATCH ANTENNA

The miniaturization of an antenna has been a point of concern for a long time. Much of the analysis concluded that a reduction in the size of the antenna gain and bandwidth have reduced by a percentage. It has been well established that there is a potentially lower bound to the Q component that can be reached for the antenna.

Quantitative lower Q-factor constraint may be given by

$$Q = \frac{1}{ka} + \frac{1}{(ka)^3}$$

Where ' k ' is a wave number and the given expression is true for a lossless antenna. It indicates that by decreasing the size of the Q factor antenna, the output of the antenna increases. So Q can be high at the expense of antenna output and antenna gain. There are essentially two approaches for miniaturizing the

microstrip patch antenna. The first approach is to adjust the properties of the substrate to reduce the effective wavelength of the substrate. The second approach is to increase the electrical current flow path. Several methods have been suggested to minimize the physical size of the pad, including the use of high dielectric substrates, magneto-dielectric substrates, expanding the current direction of the radiator, capacitive loading, shortening pins / walls, embedding tails around the sides, fractal PIFA and Quarter-Mode designs. Lower-frequency antennas, such as the industrial, Scientific and Medical (ISM) band, are reduced in size by these technologies, but still suffer from related disadvantages such as extremely inefficient radiators, small bandwidths and complex structures: they are also wide in size and profile relative to the increasing advance in technology. It remains a difficult challenge to obtain fast, compact and low-profile antenna architectures while retaining fair performance. This paper proposes and experimentally verifies a lightweight, low-profile textile wearable antenna. The proposed textile patch antenna with a rectangular slot and a filled strip pair is 25 percent of the reference antenna, Fig. 3. The integration of strip-line loading as well as rectangular slots allows for lower frequency operation, with a substantial reduction in scale. The concept not only offers excellent operating efficiency, but also a more compact format and simplified construction compared to previous versions.

In Section 2, it addresses and describes the practical architecture and method of the proposed wearable textile antenna. Section 3 sets out the analytical approach, and the final equivalent circuit is elaborated. Section 4 reviews the performance and characteristics of the design, with conclusions in Section 5.

2. ANTENNA DESIGN AND APPROACH

The antenna architecture was initially based on traditional microstrip rectangular patch antenna construction techniques and designed to work at 2.4 GHz using CST Microwave Studio R. A basic conventional microstrip rectangular patch antenna design is given below in fig 2.

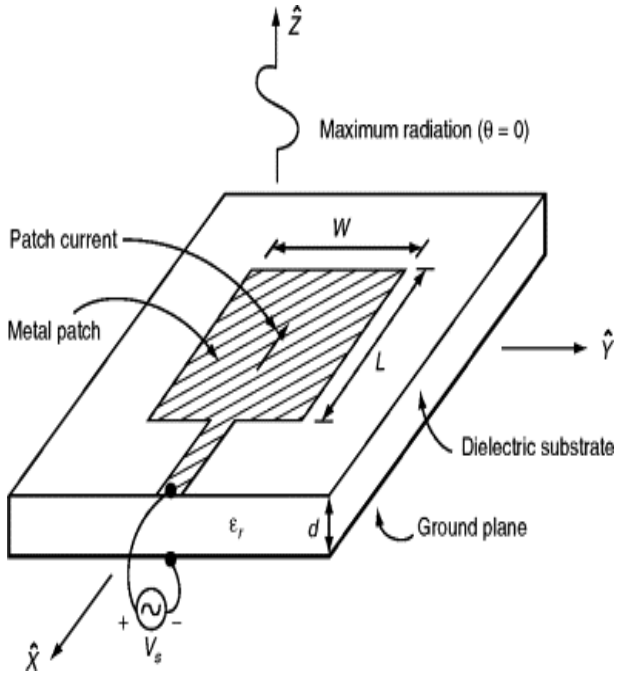

Fig 2. Conventional Microstrip Rectangular Patch Antenna Design

Consider the reference textile antenna of Fig 3 in order to allow comparisons , with width and lengths of 40 mm and 60 mm respectively.The ground plane is 12.4 mm in thickness. The Shield tTM conducting material is implemented on a 0.7 mm thick denim substrate with a low dielectric constant of 1.7, and the textile antenna patch is fed by a 50Ω microstrip line. The size of this antenna is high relative to current advancements in the miniaturization of wearable sensors.

The present work therefore aims to reduce the antenna size to half of the antenna of reference, to achieve reliable operation at the optimal operating frequency with reasonable performance.

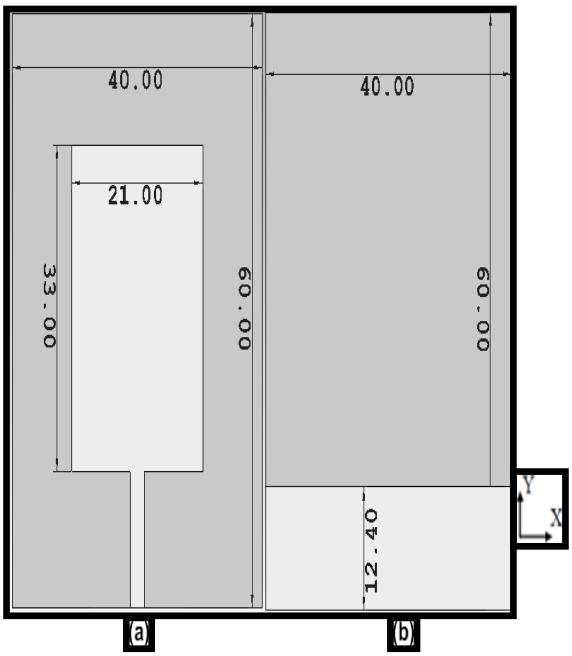

Fig 3. Reference Antenna (a) Front view (b) Back view

As mentioned above, inserting a slot (or notch) is a technique used for miniaturization of the antenna. For the specified shape and size of the radiating area, cutting holes on the surface will redirect the current propagation and increase the effective current path length. Thus, the resonant frequency will be decreased, giving an antenna output of a greater physical dimension, and the bandwidth of the antenna will be increased as the slots lower the Q value.

The antenna underwent many evolutions in order to achieve the miniaturized configuration seen in Fig. 4. In order to obtain compactness, the total dimension is reduced to half as defined by Ant. 1 in Fig. 4 (a). The slot on the upper right side of the radiating pad appears in Ant. 2, Fig. 4 (b) It increases the length of the current path and thus reduces the resonant frequency.

An adjacent slot is added on the same profile to create an E-shaped radiant mask - see Ant. 3 in Fig. 4 (c). In Fig. 4 (d), a slot in antenna's bottom right of antenna 3 is chipped off and substituted with an reversed S-shaped slot with two small lines which are kept at the center of each slot to reduce the resonant frequency further, as in Fig. 5.

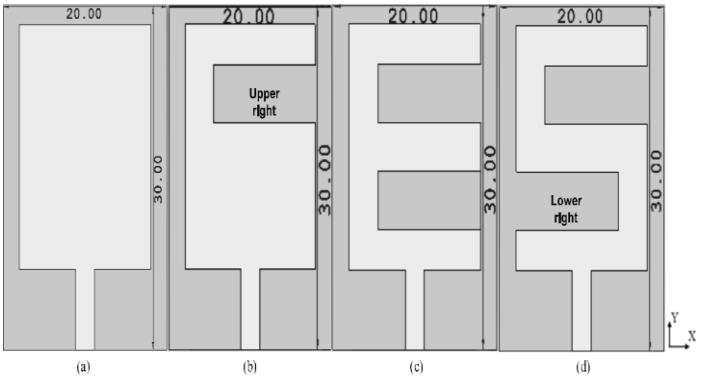

Fig 4. Evolution of the proposed antenna. (a) Ant. 1. (b) Ant. 2. (c) Ant. 3. (d) Ant. 4.

Return losses for antennas of Fig. 4 and Fig. 5 are reviewed in Section 3 the ground plane is the same size in all cases.

The antenna underwent many evolutions in order to achieve the miniaturized configuration seen in Fig.. 3. To obtain compactness, antenna reduces the total dimension to half as shown by Ant. 1 in the fig . 3 (a) (a). The space on the upper right side of the radiant layer that appears in the Ant. 2, Fig. 3(b) increases the length of the current direction and thus reduces the resonant frequency.

An extra slot is added on the same face to create an E-shaped radiating surface. see Ant. 3 in Fig. 3 (c). In Fig. 3 (d), the slot in the bottom right of Ant. 3 is taken off and substituted by reversed slot to form an S shape, with two thin lines inserted at the center of each slot, to reduce the resonant frequency furthers, as in Fig. 4. The return losses for all the antennas of Fig. 3 and Fig. 4 are

reviewed in Section 3 : the ground plane is the same size in all cases.

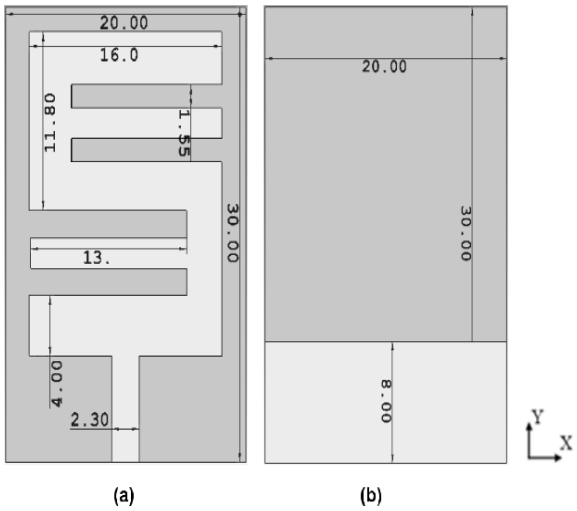

Fig 5. Antenna proposed (Ant.5) (a) Front view (b) Back view [2].

3. EQUIVALENT CIRCUIT

The identical circuits for all antennas can be seen in Fig. 6(a) 6(d). The typical rectangular simple tex-tile patch antenna can be programmed as a standard parallel RLC resonant circuit seen in Fig. 6(a).The distribution of current of standard patch travels from the feed point to the upper and lower edges of the sheet.

Furthermore, when a rectangular slot is included into the patch as shown in Fig. 4(a) the resonant features vary as shown in Fig. 6(b), as two current components stream in the radiating patch; (i) the normal current that flows for any conventional patch; and (ii) a meandered current owing around the slot, thus upgrading the current path Under this situation, all magnetic and electrical forces are discontinuous around the opening, adding all inductance and capacitance as seen in Fig. 6(b). These results have been described as series capacitance , ΔC1, and series inductance, ΔL1, additional to the equivalent circuit for a conventional microstrip patch antenna as in Fig. 4 (b).

Similarly, another extra rectangular slot (see Fig. 3(d)) will introduce another additional series inductance, ΔC2, and series capacitance, ΔC2, to the equivalent circuit of Fig. 6 (b), as shown in Fig. 6(c), further decreasing the frequency. Fig. 5 depicts the configuration of an antenna when dual additional strip lines are summed, which can be described as extra capacitances, ΔCs1 and ΔCs2, in parallel with the equivalent circuit of the antenna in Fig. 6 (c). The comparable circuit of Ant 5 in Fig. 4 is depicted in Fig. 6 (d). Due to ΔCs1 and ΔCs2, the overall capacitance of the resonant circuit increases which results in operation in lower frequency. The effects of ΔL1 and ΔC1 also lead to reduction of size.

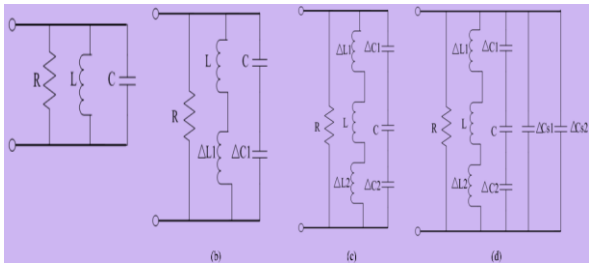

Fig 6. Comparable circuit of (a) Ant.1, (b) Ant.2, (c) Ant.4 and (d) Ant. 5.

4. ANTENNA PERFORMANCE

The reflection coeffecients when simulated using software of every antenna design shown in Fig. 3, Fig. 4 and Fig. 5 are shown in Fig. 7. Such plots gave further insight into the input of multiple-frequency spaces, making it easier to change reasonable S11 values within the working impedance bandwidth.

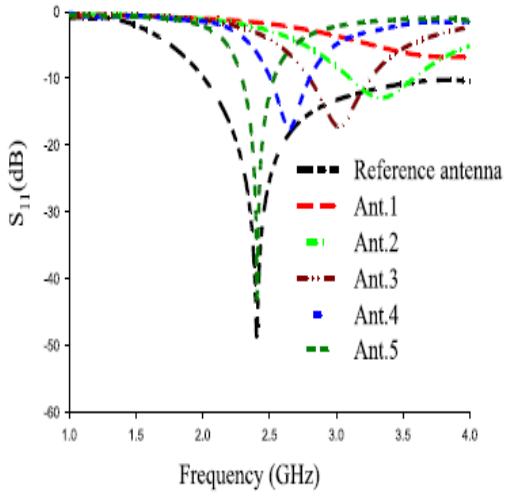

Fig 7 . Simulated reflection coefficient for various antenna configurations.

From Fig. 7, it shows that the standard antenna (Fig. 2) based on the theoretical methodology it covers a wide band of frequencies including 2.4 GHz. Moreover, it can be notified that by lowering the substrate size (see Fig. 4 (a)), S11 got shifted to high frequency of operation. Therefore, introduction of slots (Ant. 2 _ Ant. 4), S11 leads to resonate at lower frequency. The inclusion of the strip lines in Ant. 5 (Fig. 4) reduces greatly the resonant frequency of Ant. 4 (Fig. 3 (d)) towards the aimed frequency of 2.4 GHz. Along with it, Ant. 5 produces good impedance matching, and a reduction of size upto 75% compared to the reference antenna (Fig. 3).

The radiation pattern in each case is identical, with omni-directional radiation patterns in the H-plane and bi-directional radiation patterns in the E-plane. Fig.8 displays the virtual surface current distributions to help illustrate the effect of slots.

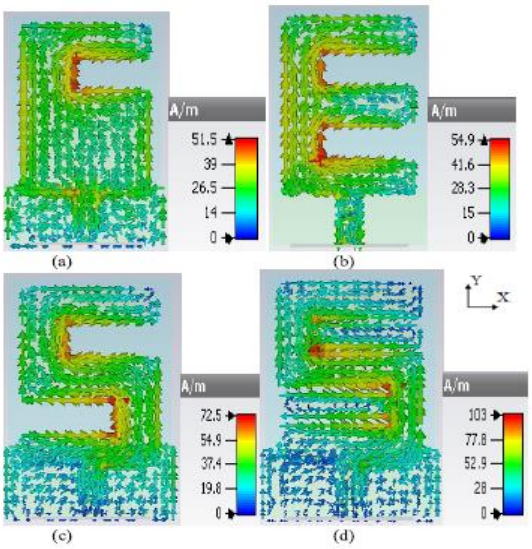

Fig 8. Simulated layer current distribution at different frequencies of antennas. (a) Ant. 3 (3.334 GHz). (b) Ant. 4 (3.022 GHz).(c) Ant. 5 (2.65 GHz). (d) Ant. 6 (2.4GHz).

The outcomes of the extra additional slots in 2, 3, 4 and 5 antennas in terms of resonances are 3.334 GHz, 3.022 GHz, 2.65 GHz and 2.4 GHz respectively. In each architecture, the highest concentrated current density is predominantly located at the slot on the pad. Slots will then adjust the resonant frequency and increase the efficiency of the antenna.

Furthermore, as the number of slots increases, the cumulative current is realized as seen in Fig.8 (d).The final equivalent circuit shown in Fig. 6 (d) is simulated and the values of each component are tabulated in Table 1.

Table 1. Bandwidth summary for various antenna configurations

Antennas	Band(GHz)	BW(MHz)	BW%
Reference Antenna	2 – 4	2000	83
Antenna 1 (a)	0	0	0
Antenna 2 (b)	3.1 - 3.5	400	11.99
Antenna 3 (c)	2.8 - 3.2	400	13.3
Antenna 4 (d)	2.5 - 2.8	300	11.3
Antenna 5 (e)	2.2 - 2.53	240	10

S_{11}(reflection coeffecient), of the equivalent circuit is in path with the outcome from CST for the antenna which is inverted E-shaped as shown in Fig. 9.

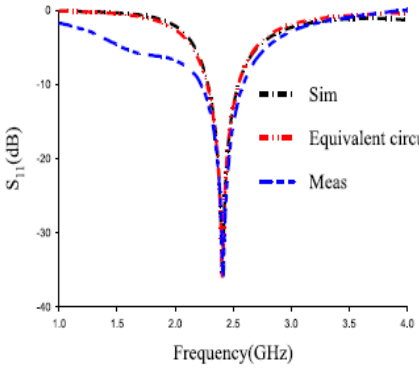

Fig 9. Measured and simulated reflection coefficient of antenna (Ant. 5).

The results of both equations are in near agreement. The antenna was built as shown in Fig. 10 and has been experimentally confirmed. The antenna reflection coefficient was evaluated and compared to the simulated and quantitative outcomes as shown in Fig. 9. Appropriate resolution shall be maintained.

On other sides, the reflection coefficient which is measured has a bandwidth wider than the simulated one, ranging from 2.23 to 2.59 GHz with 360 MHz (15%) of bandwidth, while values of the simulated ranges from 2.29 to 2.53 GHz with 240 MHz (10%) of bandwidth. This may be due to the lossy properties of the substrate material itself.

Fig. 11 compares the simulated and measured far-field radiation patterns of the antenna at E-plane and H-plane, where an adequate agreement between the two is achieved. Furtherly, slightly in the bidirectional radiation patterns in E-plane and the H-plane Omni directional patterns are obtained. Radiation patterns in both planes are normalized, this is to be noted. In addition, the antenna has a gain of 2.05 dBi.

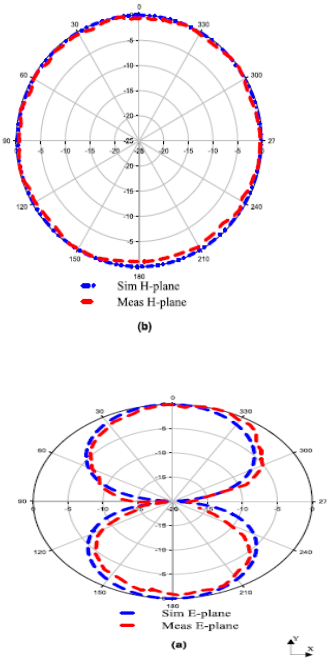

Fig 11. Simulated and measured radiation patterns of the antenna (Ant. 5): (a) E plane (b) H plane.

5. CONCLUSION

A low-profile and lightweight miniaturized antenna for 2.4GHz ISM applications has been introduced. The size is significantly reduced by filling proper rectangular slots and adding strip lines, a decrease of 75% relative to the reference antenna. The antenna has good radiation output, with around 79 per cent radiation efficiency and 15 per cent bandwidth. An analogous circuit has been developed for the proposed design and the results indicate a strong agreement with the simulations. Overall, due to its low manufacturing cost, small size and adequate radiation and bandwidth efficiency, the proposed antenna is an suitable candidate for ISM applications.

REFERENCES

[1] S. Yan, P. J. Soh, and G. A. E. Vandenbosch, ‘‘ Compact all-textile dualband antenna loaded with metamaterial-inspired structure,’’ IEEE Antennas Wireless Propag. Lett., vol. 14, pp. 1486–1489, 2015.

[2] A. Y. I. Ashyap et al., ‘‘Compact and low-profile textile EBG-based antenna for wearable medical applications,’’ IEEE Antennas Wireless Propag. Lett., vol. 16, pp. 2550–2553, 2017.

[3]A.Y.I.Ashyap,Z.Z.Abidin,S.H.Dahlan,H.A.Majid,M.R.Kamarudin, andR.A.Abd-Alhameed,‘‘Robustlow-profileelectromagneticband-gapbased on textile wearable antennas for medical application,’’ in Proc. Int. Workshop Antenna Technol. Small Antennas, Innov. Struct., Appl. (iWAT), 2017, pp. 158–161.

[4] J. Hu, ‘‘Overview of flexible electronics from ITRI’s viewpoint,’’ in Proc. VLSI Test Symp., 2010, p. 84.

[5] C. Hertleer, H. Rogier, L. Vallozzi, and L. Van Langenhove, ‘‘A textile antenna for off-body communication integrated into protective clothing for firefighters,’’ IEEE Trans. Antennas Propag., vol. 57, no. 4, pp. 919–925, Apr. 2009.

[6] J.-W. Wu, H.-M. Hsiao, J.-H. Lu, and S.-H. Chang, ‘‘Dual broadband design of rectangular slot antenna for 2.4 and 5 GHz wireless communication,’’ Electron. Lett., vol. 40, no. 23, pp. 1461–1463, Nov. 2004.

[7] R. K. Raj, M. Joseph, C. K. Aanandan, K. Vasudevan, and P. Mohanan, ‘‘A new compact microstrip-fed dual-band coplanar antenna for WLAN applications,’’ IEEE Trans. Antennas Propag., vol. 54, no. 12, pp. 3755–3762, Dec. 2006.

[8] S. Sufyar and C. Delaveaud, ‘‘A miniaturization technique of a compact omnidirectional antenna,’’ Radioengineering, vol. 18, no. 4, pp. 373–380, Dec. 2009.

[9] A. Holub and M. Polivka, ‘‘A novel microstrip patch antenna miniaturization technique: A meanderly folded shorted-patch antenna,’’ in Proc. 14th Conf. Microw. Techn., 2008, pp. 1–4.

[10] J. S. Kula, D. Psychoudakis, W. J. Liao, C. C. Chen, J. L. Volakis, and J. W. Halloran, ‘‘Patch-antenna miniaturization using recently available ceramic substrates,’’ IEEE Antennas Propag. Mag., vol. 48, no. 6, pp. 13–20, Dec. 2006.

[11] F. Farzami, K. Forooraghi, and M. Norooziarab, ‘‘Miniaturization of a microstrip antenna using a compact and thin magneto-dielectric substrate,’’ IEEE Antennas Wireless Propag. Lett., vol. 10, pp. 1540–1542, 2012.

[12] P. Salonen, L. Sydänheimo, M. Keskilammi, and M. Kivikoski, ‘‘A small planar inverted-F antenna for wearable applications,’’ in Proc. 3rd Int. Symp. Wearable Comput., 1999, pp. 95–100.